Soft X-ray Imager(SXI) onboard ASTRO-H

Kiyoshi Hayashida[a], Hiroshi Tsunemi[a], Takeshi Go Tsuru[b], Tadayasu Dotani[c], Hiroshi Nakajima[a], Naohisa Anabuki[a], Ryo Nagino[a], Shutaro Ueda[a], Takaaki Tanaka[b], Hiroyuki Uchida[b], Masayoshi Nobukawa[b], Masanobu Ozaki[c], Chikara Natsukari[c], Junko S. Hiraga[d], Hiroshi Tomida[e], Masashi Kimura[e], Takayoshi Kohmura[f], Hiroshi Murakami[g], Koji Mori[h], Makoto Yamauchi[h], Isamu Hatsukade[h], Yusuke Nishioka[h], Aya Bamba[i], Shuhei Katada[a], Kumiko Kawabata Nobukawa[b], Masachika Iwai[c], Keisuku Kondo[c], Tukasa Takeyoshi[h], John P. Doty[j] and the ASTRO-H SXI team

[a]Department of Earth and Space Science, Graduate School of Science, Osaka University, Machikaneyama, 1-1, Toyonaka, Osaka 560-0043, Japan;
[b]Department of Physics, Graduate School of Science, Kyoto University, Sakyo-ku, Kyoto 606-8502, Japan;
[c]Institute of Space and Aeronautical Science, JAXA, 3-1-1, Yoshinodai, Sagamihara, Kanagawa 229-8501, Japan;
[d]Research Center for the Early Universe, University of Tokyo, Tokyo 113-0033, Japan;
[e]ISS Science Project Office, Institute of Space and Aeronautical Science, JAXA, Ibaragi 305-8505, Japan;
[f]Department of Physics, Tokyo University of Science, Noda, Chiba 270-8510, Japan;
[g]Department of Information Science, Tohoku Gakuin University, Miyagi 981-3193, Japan ;
[h]Faculty of Engineering, University of Miyazaki, Miyazaki 889-2192, Japan;
[i]Department of Physics and Mathematics, Aoyoama Gakuin University, Kanagawa 252-5258, Japan;
[j]Noqsi Aerospace, CO 80470 , USA

ABSTRACT

Soft X-ray Imager (SXI) is a CCD camera onboard the ASTRO-H satellite which is scheduled to be launched in 2015. The SXI camera contains four CCD chips, each with an imaging area of 31 mm×31 mm, arrayed in mosaic, covering the whole FOV area of $38' \times 38'$. The CCDs are a P-channel back-illuminated (BI) type with a depletion layer thickness of 200 μm. High QE of 77% at 10 keV expected for this device is an advantage to cover an overlapping energy band with the Hard X-ray Imager (HXI) onboard ASTRO-H. Most of the flight components of the SXI system are completed until the end of 2013 and assembled, and an end-to-end test is performed. Basic performance is verified to meet the requirements. Similar performance is confirmed in the first integration test of the satellite performed in March to June 2014, in which the energy resolution at 5.9 keV of 160 eV is obtained. In parallel to these activities, calibrations using engineering model CCDs are performed, including QE, transmission of a filter, linearity, and response profiles.

Keywords: X-ray CCD, P-channel, Back-illumination, ASTRO-H, SXI

1. INTRODUCTION

ASTRO-H[1,2] is an X-ray observatory scheduled to be launched in 2015. It will carry four kinds of detectors; the Soft X-ray Spectrometer (SXS),[3–5] the Soft X-ray Imager (SXI),[6,7] the Hard X-ray Imager (HXI),[8,9] and the Soft Gamma-ray Detectors (SGD).[10,11] The former two, SXS, and SXI will be installed on the focal planes of

Further author information: (Send correspondence to K.H.)
K.H.: E-mail: hayasida@ess.sci.osaka-u.ac.jp, Telephone: (+81)-6-6850-5476

Space Telescopes and Instrumentation 2014: Ultraviolet to Gamma Ray, edited by Tadayuki Takahashi, Jan-Willem A. den Herder, Mark Bautz, Proc. of SPIE Vol. 9144, 914429 · © 2014 SPIE
CCC code: 0277-786X/14/$18 · doi: 10.1117/12.2054575

the Soft X-ray Telescope, SXT-S and SXT-I,[12,13] respectively. The HXI will be placed on the focal planes of the two sets of the Hard X-ray Telescopes (HXT),[14,15] while the SGD are non-imaging detectors with collimator.

One of the main purposes of ASTRO-H is high resolution (5 eV resolution) spectroscopy of X-ray sources at soft X-ray band (0.3-12 keV), which is primarily enabled by the SXS, micro-calorimeter. However, since the SXS field of view (FOV) is limited to $3' \times 3'$, information of the X-ary sources in the surrounding region is always needed to extract the spectrum of the target source properly. Wide ($38' \times 38'$) FOV of the SXI, even with moderate energy resolution, will take the role for it. The wide FOV of the SXI, together with low and stable background as for the Suzaku XIS, is also ideal for observations of diffuse sources with low surface brightness. Another important point of ASTRO-H is in its wide energy band, from 0.3 to 600 keV. Efficiency of the SXI will be as high as 77% at 10 keV and will have enough overlap energy band with that of the HXI. These points are essential to obtain wide energy band spectra of hard X-ray sources.

We fabricated the engineering model (EM) of the SXI in 2012, and performed various tests.[6,7] Most of the SXI flight model (FM) components were fabricated and assembled in 2013, and an end-to-end test was performed in December 2013 and January 2014. It followed by the first integration test of the ASTRO-H satellite, in which SXI was installed on the satellite from March to June 2014. In parallel to the fabrication and verification of the SXI FM, various calibrations and qualifications were performed using tje SXI EM CCDs. We report these activities and the current status of the SXI development in this paper.

2. SXI SYSTEM : DESIGN OVERVIEW

The SXI consists of a camera body (SXI-S), pixel processing electronics (SXI-PE), digital electronics (SXI-DE), and a cooler driver (SXI-CD). The SXI-S contains 4 CCD chips fabricated by Hamamatsu Photonics K.K. (HPK). The CCDs are cooled down to -110°C or -120°C with mechanical coolers. Driver electronics are installed in a box aside the camera body, while video electronics are inside the camera body. These SXI components are illustrated and schematically shown in Fig. 1.

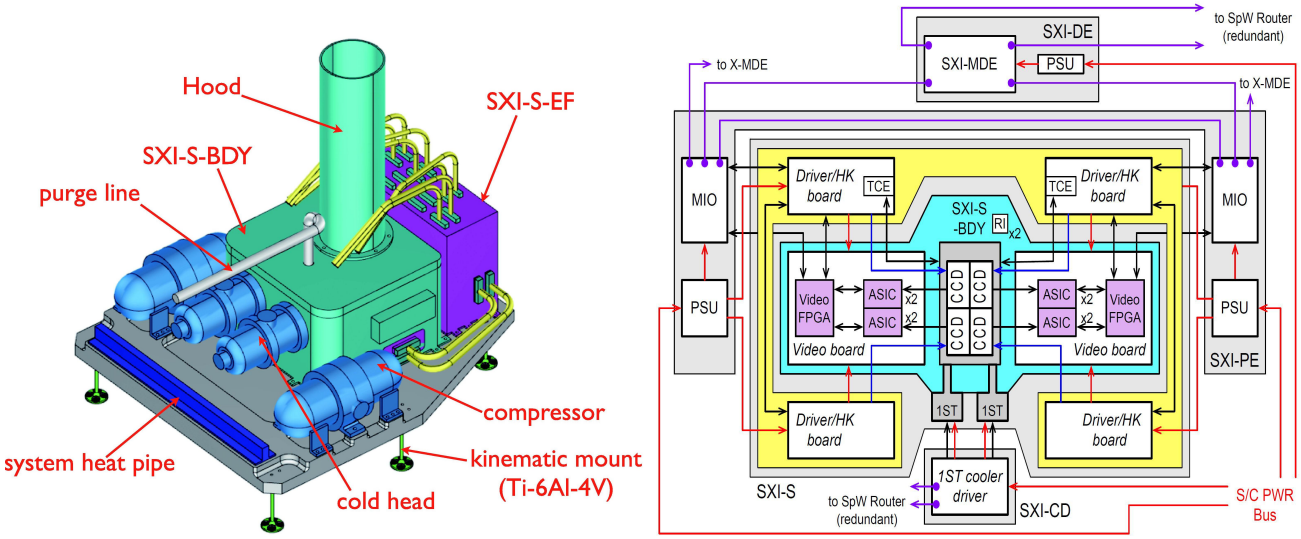

Figure 1. Left : The outlook of the SXI-S. There are 4 CCDs inside the SIX body (BDY) just below the Hood. Right : The block diagram of the SXI system. There are four sub-parts in the SXI: SXI-S, SXI-DE, SXI-PE and SXI-CD.

Design of the SXI was described in previous papers.[6,7,16,17] No major changes were applied from the SXI EM to the SXI FM, although the FPGA logic and on-board software were updated.

2.1 CCD

The SXI employs P-channel, back-illuminated (BI) type CCD, Pch-NeXT4, manufactured by Hamamatsu Photonics K.K.. Its specification is summarized in Table 1, and those installed in the SXI FM are shown in Fig 2.

The P-channel CCDs are made from N-type silicon wafers, which leads to a thick depletion layer of 200 μm. High quantum efficiency (QE) around 10 keV or higher is important to have energy band overlap with the HXI. We also consider that the SXI CCD should be BI type, not only for good quantum efficiency to low energy X-rays but also for protection against micro-meteorite impacts. Fig. 3 show the QE model of the Pch-NeXT4. In this model, transmission of the optical blocking layer (OBL) on the SXI (Al 100 nm thickness), and that of the CBF (polyimide 200 nm and Al 30 nm) are takein into account.

A proto-type of Pch-NeXT4 is Pch-2k4k, which are used in the Hyper Supreme Camera for the Subaru telescope. One drawback of the proto-type P-channel CCD had been its low energy response; a significant low energy tail was observed to soft X-ray incidence. Nevertheless, as described in Ueda et al.,[18,19] introducing an alternate treatment on the Si-interface layer, which is at the surface of the illumination (back) side, succeeded in reducing the tail by one order of magnitude. The same treatment was adopted for the EM and FM CCDs of the SXI, and reduced low energy tail was confirmed in the experiment, as mentioned below.

Table 1. Specifications of the CCD Pch-NeXT4 and its Nominal Operation Parameters for the SXI

Pch-NeXT4	CCD Configuration	Frame Transfer, BI, P-channel
	Imaging Area Pixels	1280 × 1280
	Imaging Area Size	30.72 mm × 30.72 mm
	Imaging Area Pixel Size	24 μm × 24 μm
	Silicon Thickness	200 μm
	Clock Phase	2
	Readout Nodes	4 (nominally use 2)
	Surface Coat	Al
Nominal Operation	Frame Time	4 s
	On-chip Binning	2 × 2
	CCD Temperature	−120°C∼ −110°C

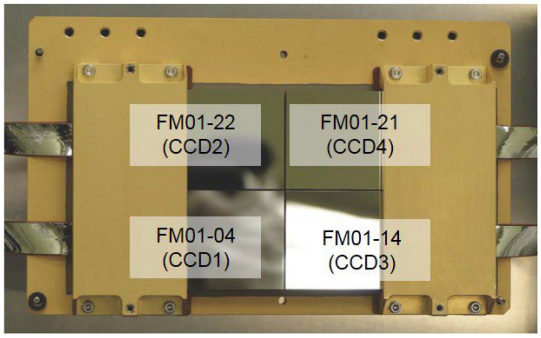

Figure 2. SXI FM CCDs installed on the cold plate, consisting of the FPA in the SXI FM Camera. CCD IDs are overlaid in the picture.

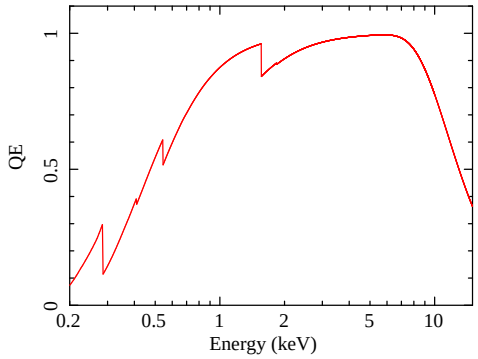

Figure 3. QE model of the SXI CCD Pch-NeXT4. The transmission of the optical blocking layer on the SXI (Al 100 nm thickness), and that of the contamination block filter (polyimide 200 nm and Al 30 nm) are taken into account.

2.2 Camera Housing and Coolers

The SXI camera housing contains the focal plane assembly (FPA) including 4 CCDs, video boards, and the one stage Stirling (1ST) coolers. At the top of the SXI housing, a bonnet and a hood are placed. The contamination blocking filter (CBF) is installed at the boundary of the bonnet and the hood. Total weight of the SXI camera body including the front end electronics are about 41 kg. Since the CCDs are one of the coolest part inside the camera body, special care is needed against contaminations. Therefore, the inside of the housing is separated into two rooms, one for the FPA and the other for the video boards.

2.3 Analog Electronics

The front end electronics (FE) take the role of a CCD driver, house keeping (HK) measurement electronics, and the FPA heater controller. The driver output is optimized for the SXI CCD, Pch-NeXT4. For example, a back bias voltage up to +40 V can be applied. Four FE boards are installed in a box aside the camera body.

On the other hand, the role of the video board is to process analog signals from the CCD and to transfer digitized pixel levels to the SXI-PE. The main part of the video signal processing is conducted by the ASICs MND02.[20,21] One MND02 ASIC accepts signals from the 4 readout nodes of a CCD, while we employ 2 ASICs for one CCD. This is for redundancy and also for noise reduction by taking average of the outputs from 2 ASICs. Besides the ASICs, FPGAs are installed on the video board. Decimation filter process is the main role of these FPGAs.

2.4 Digital Electronics

The SXI-PE consists of two FPGA boards, called Mission I/O (MIO) boards, and the Power Supply Unit (PSU). As shown in Fig. 1, the SXI-PE is connected to the analog electronics through LVDS lines and power lines. The SXI-PE functions not only as a digital processor for the pixel data from the video boards, but also takes the role of a CCD sequencer, power supply to analog electronics, commander to analog electronics, and an HK data collector. More detailed description but for the proto-type is given in by Ozaki et al.[22] and Fujinaga et al.[23]

The SXI-DE is a CPU board, called Mission Digital Electronics (MDE), that interfaces the satellite system and the SXI system, i.e., receiving the commands and transmitting them to the SXI-PE, transferring the edited data to telemetry. The communication of the SXI-DE to the SXI-PE and to other satellite system components are through Space Wire (SpW).

The hardware and basic part of the logic and software for the MIO and MDE boards are common for all the ASTRO-H mission instruments. In fact, one backup MDE called XMDE is installed on the satellite for redundancy, which will function as a substitution for any of the MDEs prepared for each subsystem.

3. PERFORMANCE VERIFICATION AND CALIBRATIONS

As mentioned above, most of the FM components of the SXI were fabricated and assembled in 2013. We describe activities to build the FM and its verification, and calibrations sine with the FM but mostly with the EM.

3.1 Basic Performance of the CCDs in the SXI

All the FM candidates Pch-NeXT4 CCDs manufactured by HPK were tested at Osaka University. The test includes X-ray irradiation with ^{55}Fe sources, O-K and Si-K lines from a system consisting of a target plus a soft X-ray electron impact source, and optical light irradiation. The optical light irradiation was included to verify the OBL covers whole the CCD area. We scored the candidates CCDs by various aspects of performance, and the four CCDs with highest scores were selected and installed on the FPA of the SXI FM.

We performed an end-to-end test of the SXI-S almost full FM in December 2013 and January 2014. The CCDs were cooled down by SXI-1ST down to -120°C. We confirmed that the stability of the temperature control is less than 0.2°C. With nominal drive clock settings and averaging two ASICs inputs for each read out node, we obtained readout noise of 5 e^- to 7 e^-. The gain is 5.8 eV/ch to 6.8 eV/ch, depending on the nodes. The readout noise is slightly smaller than that measured in various experiments in the development phase when the video board were placed outside the camera housing with a longer cable. The SXI FM was then installed on the satellite, and joined the first integration test of the satellite in March to June 2014. In June 2014, we performed an end-to-end test again with SXI-PE FM, as shown in Fig. 4.

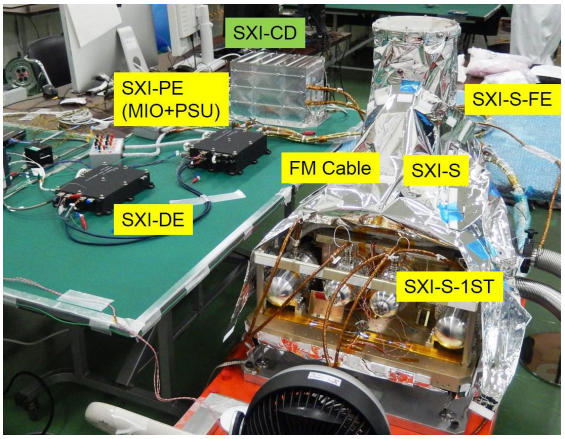

Figure 4. End-to-End Test of the SXI FM system performed at Tsukuba Space Center, JAXA on 2014 June. SXI components are FM except for SXI-CD. The CCDs were cooled down to -120°C$\sim -110^{\circ}$C, and were irradiated with X-rays from ^{55}Fe sources. In order to make the camera body vacuum tight, we replaced the FM bonnet with a vacuum tight flange.

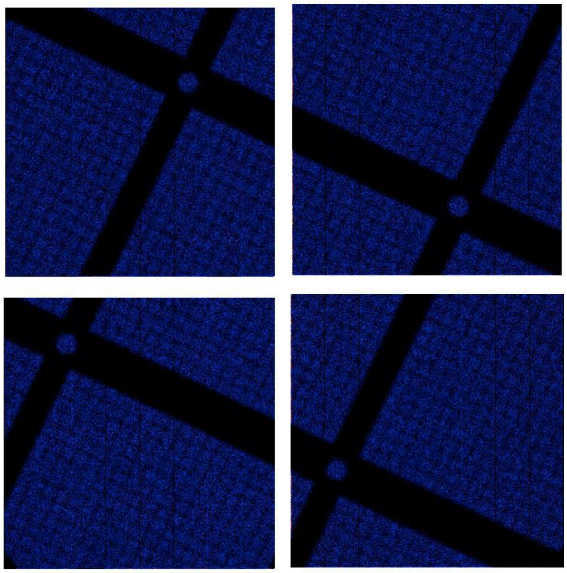

Figure 5. X-ray image of the mesh in front of the SXI FM CCD. X-rays from ^{55}Fe were irradiated. The bottom left, top left, bottom right, top right are CCD1, CCD2, CCD3, and CCD4, respectively. Look down view.

3.2 Measurement of the CCD Alignment with a Mesh

We measured the alignment of the CCDs by placing a metal mesh in front of the CCDs. X-rays from ^{55}Fe source were irradiated to make a shadow of the mesh on the CCDs. Fig. 5 shows the X-ray image taken in the experiment. The relative alignment of the four CCD chips was accurately (much finner than a pixel size) determined for the pattern of the mesh to be aligned. The gaps between the CCDs are , corresponding to $36'' - 45''$ on the focal plane. Note that the values of the gaps include inevitable dead space at the edges of each CCD package. Alignment of the CCDs will be verified in orbit by observing X-ray sources on the sky.

3.3 Charge Injection and CTI Correction

Radiation damage is inevitable for the CCDs in orbit. Among various modes of the damages, increase in the charge transfer inefficiency (CTI) is the most serious one for the X-ray CCDs. We studied the radiation tolerance of the SXI EM CCDs by irradiating high energy protons at the Tandem accelerator in Kyushu University. The proton energy incident to the CCD was 6.7 MeV. With this energy, protons provide fairly flat energy deposit over the CCD depth, about 12-18 keV/μm. This energy deposit in the CCD was much larger than the case with conventionally used 20-40 MeV case. As described in Mori et al.[24] the degradation in the CTI for the SXI CCDs is comparable to the Suzaku XIS CCDs. The CTI is lower for lower temperatures in the range from -140°C to -60°C.

As also shown in Mori et al.,[24] spaced-row-charge injection (SCI) is effective to reduce the CTI by factor of two. Since the CTI of the SXI FM CCDs was not negligible, $0.9\text{-}1.5\times10^{-5}$/vertical-transfer according to the measurement in the screening test, we employ the SCI for the SXI from the beginning of the mission.

Application of the SCI to the SXI EM CCD is described in Nobukawa et al.[25] The EM CCD used in the experiment had a relatively high CTI and yielded Grade02346 FWHM at 5.9 keV of 220 eV. Introducing the SCI improved the resolution to 184 eV, although gain non-uniformity of 0.5% remains like thaw-tooth structure along the vertical transfer. Further improvement was achieved, i.e., FWHM of 180eV and gain non-uniformity of 0.1%, by applying trail correction and residual CTI correction, both of which were established in the data processing on the ground for the Suzaku XIS. With the SXI FM system installed on the satellite during the first integration test operated with the CCD temperature of -110°C, we obtained the Grade 02346 FWHM of 174 eV

in the segment CD of CCD4 with SCI but without the residual CTI correction. Application of the residual CTI correction led to the FWHM of 160 eV, as shown in Fig. 6 We consider this will be typical values for that at the beginning of the mission.

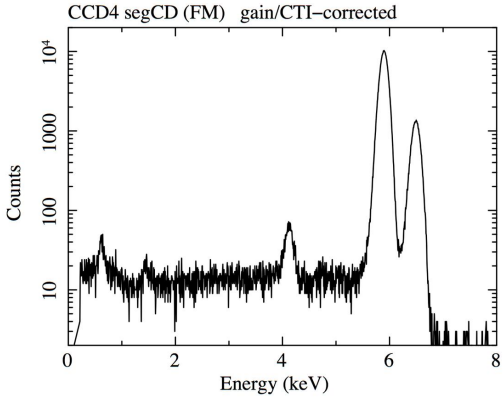

Figure 6. X-ray spectrum of ^{55}Fe obtained with the SXI FM installed on the satellite during the first integration test. The spectrum is all the X-ray grades, Grade02346, extracted from the segment CD of the CCD4. CCD temperature was −110°C, SCI was employed, and the residual CTI correction was applied. The energy resolution FWHM for 5.9 keV Mn-Kα line is 160 eV.

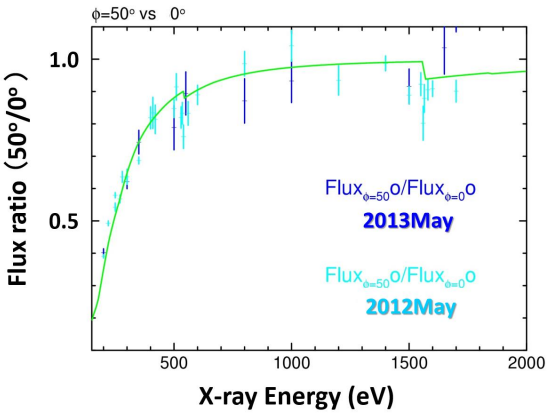

Figure 7. Ratio of the number of the events detected with a SXI mini CCD for 50° incidence to that in 0° incidence, as a function of incident X-ray energy. The ratio reflects the soft X-ray QE of the CCD. The model curve is not derived by fitting but from the design values.

3.4 QE and Filter Transmission Measurement

High QE over wide energy band is one of the most important characteristics of the SXI CCD. QE at high energy band is mainly determined by the thickness of the depletion layer. In the case of the SXI CCD, detection of soft (<1 keV) X-rays assures the fact that the device is fully depleted.

On the other hand, the QE at low energy band is primarily determined by the dead layer on the incident surface. Optical blocking layer (OBL) is an apparent dead layer. We have measured the soft X-ray QE of the mini size CCD manufactured with the same manner as the SXI CCDs at synchrotron facility, KEK-PF BL-11A. Measurement of the absolute QE at soft X-ray energies is difficult as no good reference counters is prepared. We thus employed the slant incident method developed for soft X-ray calibration of CCDs.[26] The ratio of detected X-ray flux of 50° incidence to 0° incidence is plotted as a function of X-ray energy in Fig. 7. The data points are still preliminary but the model curve based on the design value reproduces the result.

The X-ray transmission of the contamination blocking filter (CBF) was accurately measured by employing synchrotron facility, either. The X-ray absorption fine structures (XAFS) of filter material are also measured, as described in Kohmura et al.[27]

3.5 Response to Various Energy X-rays

Most of the performance verification of the SXI FM has been conducted with ^{5}5Fe sources, while we irradiated the FM CCD with X-rays of O-K and Si-K lines in their screening process. We also performed experiments with the EM CCD and mini-sized CCDs to measure response to various energy X-rays. Nobukawa et al. studied energy to pulse height relation, showing linearity is good.[25] Fluorescent X-rays from various materials will be used in the FM calibration scheduled in August 2014, too.

Our previous concern with prototype CCDs has been a significant low energy tail in their soft X-ray response. As described in Ueda et al.,[19] we succeeded in reducing the low energy tail in a test Pch BI CCD by an alternate surface treatment. The same treatment was applied to the SXI EM and FM CCDs. We confirmed the low energy

tail is as small as those reported in Ueda et al.[19] Fig. 8 shows the Grade02346 spectrum to O-K, Si-K, and Mn-K irradiation in the FM CCD screening. There are some contribution from C-K and Mg-K. Response is basically approximated with three components. Two Gaussian lines (primary and secondary) consisting the main peak and a flat tail. Modeling the response is in progress to establish the response function available for users.

We also have special concern about the X-ray response of the SXI CCDs in the energy range around Si-K edge. On this part, the response of the Suzaku XIS have a problem that significant residual remains. We hence performed an experiment at a synchrotron facility using a mini size CCD to examine the response in detail. We observed the tail is significantly smaller for the X-rays of which energy is below Si-K edge. This is reasonable if the tail component is originated in the surface layer and charge loss in that layer. The detailed result will be reported elsewhere.

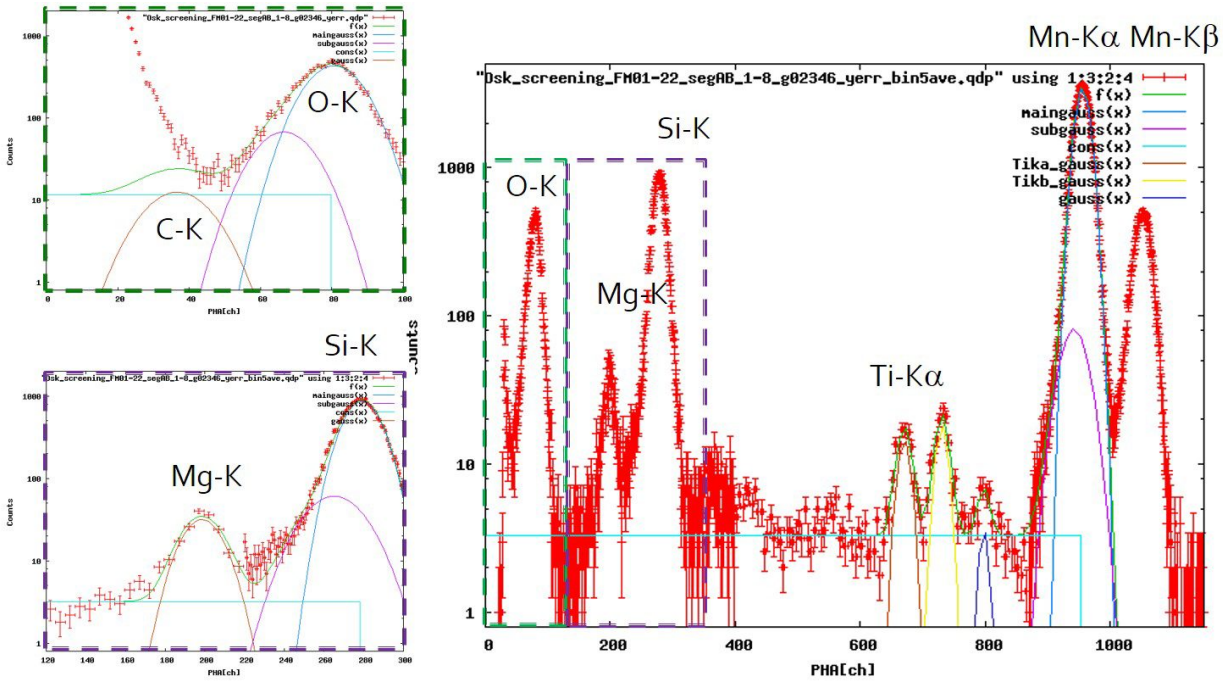

Figure 8. X-ray spectrum obtained in the SXI FM CCD screening. Low energy tail is seen in the response but more than one order of magnitude smaller than that in the proto-model CCDs. We approximate the response profile for single energy incidence with three components.

4. SUMMARY

We completed the almost full FM SXI and performed a end-to-end test. The SXI FM system was then installed on the satellite in its first integration test in March to June 2014. The SXI system functioned well; readout noise of $5\,e^-$ to $7\,e^-$ and FWHM at 5.9 keV of 160 eV were obtained. Overall, no major problems were found. FM calibration with various energy X-rays is planned in August 2014, followed by various environment tests of the system and final integration test of the satellite until the launch at the end of 2015.

ACKNOWLEDGMENTS

We acknowledge the support from Hamamatsu Photoics K.K, Mitsubishi Heavy Industry K.K., and Sumitomo Heavy Industry K.K.. KH acknowledge the support from the Grant-in-Aid for Scientific Research 23340071 and 26109506, HT from that of 230000040, and HN from that of 24684010.

REFERENCES

[1] T. Takahashi et al., "The ASTRO-H X-ray Observatory," *Proceedings of SPIE* **8443**, 84431Z–84431Z–22 (2012).

[2] T. Takahashi et al., "The ASTRO-H X-ray astronomy satellite," *Proceedings of SPIE* **9144**, in press (2014).

[3] K. Mitsuda et al., "The High-Resolution X-ray Microcalorimeter Spectrometer System for the SXS on ASTRO-H," *Proceedings of SPIE* **7732**, 773211–773211–10 (2010).

[4] K. Mitsuda et al., "Soft x-ray spectrometer (SXS): the high-resolution cryogenic," *Proceedings of SPIE* **9144**, in press (2014).

[5] M.E. Eckert et al., "Detector system ground calibration of the astro-H soft x-ray," *Proceedings of SPIE* **9144**, in press (2014).

[6] K. Hayashida et al., "Soft x-ray imager (SXI) onboard ASTRO-H," *Proceedings of SPIE* **8443**, 844323–844323–9 (2012).

[7] H. Tsunemi et al., "Soft x-ray imager onboard ASTRO-H," *Proceedings of SPIE* **8859**, 88590C–88590C–9 (2013).

[8] M. Kokubun et al., "Hard X-ray Imager (HXI) for the ASTRO-H Mission," *Proceedings of SPIE* **8443**, 844325–844325–15 (2012).

[9] G. Sato et al., "The hard x-ray imager (HXI) for the ASTRO-H mission," *Proceedings of SPIE* **9144**, in press (2014).

[10] S. Watanabe et al., "Soft gamma-ray detector for the ASTRO-H Mission," *Proceedings of SPIE* **8443**, 844326–844326–19 (2012).

[11] Y. Fukazawa et al., "Soft gamma-ray detector (SGD) onboard the ASTRO-H mission," *Proceedings of SPIE* **9144**, in press (2014).

[12] T. Okajima et al., "First measurement of the ASTRO-H soft x-ray telescope performance," *Proceedings of SPIE* **8443**, 844320–844320–8 (2012).

[13] Y. Soong et al., "ASTRO-H Soft X-ray telescope (SXT)," *Proceedings of SPIE* **9144**, in press (2014).

[14] H. Awaki et al., "Current status of ASTRO-H Hard X-ray Telescopes (HXTs)," *Proceedings of SPIE* **8443**, 844324–844324–8 (2012).

[15] H. Awaki et al., "ASTRO-H Hard X-ray telescope (HXT)," *Proceedings of SPIE* **9144**, in press (2014).

[16] H. Tsunemi et al., "Soft X-ray Imager (SXI) Onboard ASTRO-H," *Proceedings of SPIE* **7732**, 773210–773210–11 (2010).

[17] K. Hayashida et al., "Development of the soft x-ray imager (SXI) for ASTRO-H," *Proceedings of SPIE* **8145**, 814505 (2011).

[18] S. Ueda et al., "Development of the X-ray CCD for SXI onboard ASTRO-H," *Proceedings of SPIE* **8145**, 814504 (2011).

[19] S. Ueda et al., "Measurement of the soft X-ray response of P-channel back-illuminated CCD," *Nuclear Instruments and Methods in Physics Research A* **704**, 140–146 (2013).

[20] H. Nakajima et al., "Development of the analog ASIC for multi-channel readout X-ray CCD camera," *Nucl. Instr. and Meth. A* **632**, 128–132 (2011).

[21] H. Nakajima et al., "Single event effect characterization of the mixed-signal ASIC developed for CCD camera in space use," *Nuclear Instruments and Methods in Physics Research A* **731**, 166–171 (2013).

[22] M. Ozaki et al., "NeXT SXI data processing system," *Proceedings of SPIE* **7011**, 70112L–70112L–9 (2008).

[23] T. Fujinaga et al., "Development of the data acquisition system for the X-ray CCD camera (SXI) on board ASTRO-H," *Proceedings of SPIE* **8145**, 814503 (2011).

[24] K. Mori et al., "Proton radiation damage experiment on P-Channel CCD for an X-ray CCD camera onboard the ASTRO-H satellite," *Nuclear Instruments and Methods in Physics Research A* **731**, 160–165 (2013).

[25] K.K. Nobukawa et al., "Use of a charge-injection technique to improve performance f the soft X-ray imager aboard ASTRO-H," *Nuclear Instruments and Methods in Physics Research A* , in press (2014).

[26] K. Hayashida et al., "New calibration method for x-ray detection efficiency without using reference counters," *Proceedings of SPIE* **4851**, 933–944 (2003).

[27] T. Kohmura et al., "Soft x-ray transmission of contamination blocking filter for SXI onboard," *Proceedings of SPIE* **9144**, in press (2014).